

# Direct Detection of Dark Matter with Space-based Laser Interferometers

A. W. Adams<sup>1</sup>, J. S. Bloom<sup>1,2</sup>

<sup>1</sup> *Harvard Society of Fellows, 78 Mount Auburn Street, Cambridge, MA 02138 USA*

<sup>2</sup> *Harvard-Smithsonian Center for Astrophysics, MC 20, 60 Garden Street, Cambridge, MA 02138, USA*

## ABSTRACT

Dark matter pervades the Solar System, free-streaming at the local Galactic orbital velocity of the halo with a space density of  $\sim 9 \times 10^{-25} \text{ gm cm}^{-3}$ . As these objects pass through the Solar system, they perturb gravitationally, and thus very weakly, all nearby inertial masses. Making use of this, we propose an approach to the direct detection of dark matter at previously inaccessible intermediate masses ( $10^{14} - 10^{20} \text{ gm}$ ). Such mass scales are relevant, for example, for dark matter made of primordial black holes or clumped matter in a sequestered sector. If such dark matter exists, it will be unambiguously detectable through its inelastic gravitational interaction with the proposed Laser Interferometer Space Antenna (LISA) experiment. We demonstrate the efficacy of this approach by studying the dark matter signal in numerical simulations of the LISA data stream. A more conservative approach — to detect dark matter in the differential acceleration power spectrum — significantly underestimates the expected rates for LISA. Interestingly, while the space-density of  $10^{15} \text{ gm DM}$  objects would be comparable to the space-density of asteroids of similar masses, such “light matter” contaminants are readily detectable in reflected Solar light, allowing for the elimination of the major background contaminant.

*Subject headings:* dark matter — instrumentation: interferometers — techniques: interferometric — gravitation

## 1. Introduction

Only a small fraction of the mass in the universe has been directly detected through its electromagnetic signature; the existence of the remaining dark matter (Zwicky 1933) is inferred from its gravitational fingerprint. This dark matter is believed to comprise a

free-streaming gas of massive objects whose detailed nature is largely unconstrained; viable models posit masses anywhere between a few electronvolts and millions of solar masses. Searches on both the high (Alcock et al. 2001) and low (Hagmann et al. 1998) ends have so far led to no convincing account for the missing mass in the universe. Dark matter is the dominant component of the gravitational potential of galaxy clusters, galaxies, and perhaps galactic disks (Tremaine 1992; Carr 1994). Searches for Galactic halo gravitational microlensing (Paczynski 1986) of planet-mass (and larger) dark matter suggest that no more than  $\sim 40\%$  of the baryonic component of dark mass in the Galaxy can be contained in such compact objects (“MACHOs”) with masses from  $10^{26} - 10^{34}$  gm (Alcock et al. 2001). On particle physics scales, searches for weakly interacting massive particles (WIMPs) have thus far produced only negative results — however, these experiments assume weak non-gravitational couplings to ordinary matter, and so offer no bounds on purely gravitationally-coupled dark matter. Dark matter on mass scales less than  $10^{25}$  gm have never been searched for through gravitational interactions.

From matching observations to theory (Blumenthal et al. 1984; Davis et al. 1985; de Bernardis et al. 2000), it is believed that dark matter comprises a free-streaming (non-interacting) fluid of cold (non-relativistic) compact objects. The nature of the constituents of this cold free-streaming fluid is almost completely model dependent. The possible origins of DM at the high and low mass range have been reviewed elsewhere (Griest 1995; Afshordi et al. 2003; Bertone et al. 2004). At intermediate masses, there are two broad classes of popular DM candidates. First, it is possible that a large fraction of this fluid is composed of microscopic primordial black holes (PBHs) (Hawking 1971; Carr & Hawking 1974; Clancy et al. 2003); the mass scale for these is set by the dual requirement that (a) they comprise a significant fraction of the inferred dark matter energy density, and (b) were created (at some point well before Big Bang Nucleosynthesis) at sufficiently high mass that the majority have not yet Hawking-evaporated (Hawking 1975); this suggests that surviving PBH have masses, very roughly, somewhere over  $10^{15}$  gm. Secondly, the dark matter could be formed of non-baryonic matter typical in models with extra dimensions, for example fields on a distant brane in string theory (Arkani-Hamed et al. 1999); since the physics of such purely gravitationally-coupled systems is, by definition, beyond our ability to constrain from non-gravitational observations, in this paper we take the maximally agnostic stance that such systems might produce compact objects on any mass scale, relying on observations to rule them out.

Ontology aside, Galactic halo constituents of any mass are thought to be isotropically distributed and free-streaming through the Solar System with Galactic-orbital velocity ( $v_{\text{circ}} \approx 230 \text{ km s}^{-1}$ ), with the dark mass density in the neighborhood of the Solar System equal to the local Galactic halo density, about  $\rho_{\text{DM}} = 9 \times 10^{-25} \text{ gm cm}^{-3} \equiv \rho_{\text{DM,halo}}$  (Gates

et al. 1995). This value of  $\rho_{\text{DM}}$  is consistent with upper-limits on increased perihelion precession of Solar System bodies (Gron & Soleng 1996) ( $\lesssim 10^{27}$  gm dark matter mass contained within the orbit of Uranus). Note that with this DM density and characteristic velocity, the Sun would accrete only  $\approx 10^{-9} M_{\odot}$  dark matter over its lifetime.

It is important to emphasize the following: if DM objects couple only gravitationally to ordinary matter, they may well pervade the Solar System without ever having been noticed. For example, asteroids of masses similar to those considered herein are easily detected when colliding with a planet not because of gravitational interactions, but due to electromagnetic interactions, which result in the vaporization of the asteroid and the accompanying catastrophe for the planet. A truly *dark* asteroid, however, would sail through the planet almost as quietly as a neutrino.

## 2. Detecting dark matter with LISA

A dark matter object streaming through the Solar System will gravitationally scatter a test mass; the deflection of the orbit of this test mass is thus a direct measurement of the passage of the dark object. Since the profound weakness of gravitational interactions makes the magnitude of these deflections extremely small, our ability to detect dark objects via gravitational scattering is limited by our ability to accurately map the motion of inertial test masses.

The 5-year LISA experiment (Bender et al. 1998), due to launch in 2011, will feature three spacecraft, forming an equilateral triangle of arm length  $b = 5 \times 10^{11}$  cm, in an Earth-trailing orbit. The interferometric design calls for an rms positional accuracy of  $\sigma = 10^{-9}$  cm every sample at a rate of  $S = 1$  Hz. With such precision, the passage of a sufficiently massive body should be, in principle, easily seen: taking  $M_{\text{DM}} = 10^{15}$  gm  $\equiv M_{15}$ , the typical distance to the nearest object is  $l_{\text{typ}} \approx 10^{13}$  cm  $M_{15}^{1/3} \rho_{\text{DM,halo}}^{-1/3}$ , less than the Earth-Sun distance. If  $\vec{l}$  is chosen as the distance of closest approach (“impact parameter”), then over a timescale of  $|\vec{l}|/v \approx 5$  days ( $l/l_{\text{typ}}$ ), the dark object will effectively displace the test mass impulsively in a direction parallel to  $\vec{l}$  by  $(l/v)^2 G M_{15} / 2l^2 \approx 6.3 \times 10^{-8}$  cm, where  $G$  is Newton’s constant. This impulsive displacement over 5 days is  $\approx 60$  times the rms noise on a single 1 sec sample from LISA.

In the absence of other forces, and with long-lived coherence ( $>$  week) in absolute positioning, this signal would be rather straightforward to detect. However, two effects complicate the detection considerably. First, only the change in the separation between pairs of LISA stations is measured, so the effect of a passing DM object will only be seen

if the DM object imparts a substantial *differential* (i.e., tidal) force between two stations, that is when the impact parameter to one station is on the order of the LISA arm length or smaller. Secondly, the Keplerian orbits of the spacecraft and the presence of major Solar System bodies perturb the inter-station distances by factors of  $\sim 10^{17}$  and  $\sim 10^{13}$ , respectively, over the expected DM signal (see Figure 2).

### 2.1. Conservative Analytic Estimate of Rates: Detecting DM in the acceleration power-spectrum

A very conservative estimation of the S/N ratio of such measurements may be obtained by exploiting the well-developed techniques in the pre-phase A study for LISA (Bender et al. 1998), which calculate S/N ratios in the acceleration power-spectrum of a passing asteroid. While this is the correct technique for estimating the background due to asteroids and comets obscuring the oscillatory signal from gravitational waves, this is very far from the optimal technique for detecting impulsive near-field events, as discussed above; nonetheless, it gives a pleasingly reasonable, if unduly conservative, measure of the expected number of events. Using these techniques, we estimate that a  $(S/N) > 3$  would be obtained for an impact parameter to one spacecraft of  $l_{\max} < 4.2 \times 10^{10} \text{ cm } M_{15}^{2/3} v_{230}^{-1/3}$ , for impacts between  $6.1 \times 10^8 v/v_{230} \text{ cm} < l \lesssim b/3 = 1.7 \times 10^{11} \text{ cm}$ . Here the lower limit bounds the analytic approximation to the S/N integration (at smaller  $l$ , the value of  $l_{\max} \propto M$ ). The upper limit is imposed since at larger impact, tidal forces on LISA become important and only the *differential* acceleration can be measured. In this case, for  $l_{\max} > b/3$  we estimate the maximum impact parameter to be:

$$l_{\max} = \left[ \frac{13\pi (GMb)^2}{64(S/N)^2 v a_c^2} \right]^{1/5}, \quad (1)$$

where  $a_c = 6 \times 10^{-13} \text{ cm s}^{-2}/\sqrt{\text{Hz}}$  (see Bender et al. 1998). The value of  $l_{\max} = b/3$  when  $M \approx 3.5M_{15}$ . Thus, for passages larger than  $b/3$ , only masses greater than  $\approx 3.5M_{15}$  will produce a measurable effect in acceleration power-spectrum.

To arrive at an approximate upper bound on the expected event rate  $R(M)$  from this analysis, we assume that all DM have the same mass and that the flux of DM objects is  $f(M) = \rho_{\text{DM,halo}} v_{230}/M = 2.1 \times 10^{-32} M_{15}/M \text{ cm}^{-2} \text{ s}^{-1}$ . The value of  $R(M) = \pi l_{\max}^2 f(M)$  is  $6.4 \times 10^{-10} (M/M_{15})^{1/3} \text{ s}^{-1}$  for  $M \lesssim 5M_{15}$  and  $4.0 \times 10^{-10} (M/10M_{15})^{-1/5} \text{ s}^{-1}$  for  $M \gtrsim 5M_{15}$  (that is, the peak sensitivity of LISA using this method is around  $M_{\text{DM}} = 5 \times 10^{15} \text{ gm}$ ). Multiplying this by 3 (for each station) and by 5 years, the expected number of DM events detected in acceleration-frequency space by LISA is  $\sim 0.04$  (for  $M_{\text{DM}} = M_{15}$ ). We note that

with only a few orders of magnitude decrease in the system acceleration noise, the next generation gravitational-wave interferometer should easily detect several events, if indeed dark matter on these mass scales exists.

## 2.2. Detecting the Impulsive Signals from DM: A Simulation

It is very encouraging that the expected number of events approaches unity with the conservative measurement of S/N using acceleration power spectra. However, we emphasize that unlike LISA signals from weak gravitational waves, the DM passages by LISA are strongly inelastic, changing the optimal detection scheme in several important ways. Most importantly, the fact that the interaction is impulsive rather than oscillatory means that even when peak acceleration at nearest approach is relatively small, the net displacement may be quite large. Furthermore, since each such inelastic collision changes the circumference, such perturbations can be unambiguously attributed to near-field objects rather than gravitational waves (this center sagnac channel is actually a rejection trigger for LISA’s gravitational-wave mission). Additionally, since the major-body near-field interaction timescales are significantly longer than the timescale for lower-mass DM scattering events, the DM signal may be explicitly decoupled from major-body perturbations (see Figure 3). Finally, since the nearest-approaches to the various LISA stations are separated by  $b/v_{\text{DM}} \approx 6$  hr time lags, detecting (or predicting) such duplications in the impulsive signal provides a powerful check.

Unfortunately, the role of instrumental noise and decorrelation in determining a precise S/N measure for this impulsive-search strategy will require a new set of techniques (we leave this analysis to future work). As a first test the feasibility of this search strategy, we have run extensive simulations of the LISA experiment to determine whether such DM scattering events are in fact detectable in the LISA datastream. As will be clear from the figures, these inelastic collisions with the LISA constellation are readily seen in the impulsive signal on the inter-station timeseries on scales significantly larger than LISA’s 1 sec rms accuracy.

The simulations essentially keep track of the perturbation from their Keplerian orbits of the three LISA stations due to all relevant massive objects in the solar system. The basic LISA orbits were taken from the equations presented in Cornish & Rubbo (2003), and are recorded to second order in the eccentricity of the LISA constellation. The ”major-body” perturbations are those due to all inner Solar system planets and the Moon whose positions are determined from their known orbits.

Smaller perturbations are due to the simulated dark matter with fixed mass density  $\rho_{\text{DM}} = 9 \times 10^{-25} \text{ gm cm}^{-3}$ . We generate an isotropic distribution of DM masses, choosing

random starting positions of  $N$  DM objects in a volume  $V$  (set so that  $N = \rho_{\text{DM}} \times V/M$ ). For each DM object, a randomly oriented velocity is chosen with magnitude drawn from a Maxwellian distribution (with  $v_0 = v_{\text{circ}} = 230 \text{ km s}^{-1}$ ) truncated at the escape velocity of the Galaxy ( $v_{\text{esc}} = 600 \text{ km s}^{-1}$ ) at the Solar distance from the Galactic center (Lewin & Smith 1996). The motion of individual DM objects is assumed to be free streaming (ie., acceleration is zero) through the simulation volume, and the object is reflected through the origin once reaching the volume edge. The typical streaming time through the volume is  $\sim V^{1/3}/v \approx 30$  days. The free streaming assumption is a reasonable approximation since the escape velocity from the Solar potential at 1 AU is  $42 \text{ km s}^{-1}$  so DM trajectories on length scales  $< 1 \text{ AU}$  are not significantly altered by the stellar nor planetary potentials. The gravitational coupling between DM objects has a negligible affect on the trajectories.

As expected, the simulations reveal myriad sharp, manifestly impulsive short-timescale perturbations to the inter-station distances. Figure 1 shows the result of the perturbations from Keplerian orbit due to dark matter only. While the perturbations on a single station are large (indeed, millions of times larger than the 1 sec rms accuracy of LISA), the resultant LISA signals, ie changes in the armlengths due to tidal effects, are indeed quite small - though certainly measurable. This is an important point for future experiments, to which we shall return below. Note that for larger masses the perturbation scale is larger, but there are fewer impulse “events” on a single station.

Figure 2 demonstrates the vastly different scales of the perturbations, while figure 3 shows that despite the presence of strong perturbations from major bodies, the passage of DM objects can be detected as short time scale impulsive perturbations on the inter-station timeseries at magnitudes significantly larger than the 1 sec rms accuracy of LISA. For instance, in the  $M_{\text{DM}} = 10^{18} \text{ gm}$  simulation, we see tens of events with  $\delta d > 1 \text{ \AA}$  over  $\Delta t < 10$  days (see Figure 3b). The rate at this impulse scale decreases quickly for masses less than  $\sim 10^{15} \text{ gm}$ .

In figure 4 we show the details of a single DM event from the  $10^{14} \text{ gm}$  DM simulation. There are several important characteristics of these near-field events discussed above and demonstrated in this figure. First, the event duration is significantly shorter ( $< 1$  week) than the timescale for perturbations due to the Moon (and other major bodies). Second, the circumference changes during the event. Third, the time lag between features in the inter-station distances is less than  $\sim 2$  days, comparable to the quantity  $b/v$ . Fourth, assuming the LISA decorrelation time is a few days or longer (as expected), since the rms errors for a 24 hr timespan is smaller than the event scale, such events should easily recognizable by their significant departure from a 2nd order polynomial fit.

We consider the typical events produced by  $10^{14} \text{ gm}$  DM as the lower bound on the

detectability given the advertised LISA sensitivities. There appears to be several tens of such events in our simulation of a 5 year mission. The upper bound on the detectable mass (around  $10^{20}$  gm) is set by two considerations: a) the event rates drop at higher masses and b) the timescale for DM deflection becomes comparable to timescale for the lunar perturbations. Indeed, the maximum impact parameter for all masses, regardless of the actual noise characteristics of LISA, is roughly set by  $l_{\max} \approx v_{\text{DM}} \times 28 \text{ days} \approx 3.7 \text{ AU } v_{230}$ .

### 3. Non-dark Impulsive Backgrounds

LISA will also scatter inelastically off comets, asteroids and other minor Solar System baryonic bodies (Bender et al. 1998). The pre-Phase A study concluded that only the most massive asteroids produce signatures with  $S/N > 3$  using the acceleration power-spectrum analysis, with a rate of  $\sim 0.08$  events/yr, and are thus not a significant background for gravitational wave detection. As discussed above, we believe the detection rate will be much higher (by several orders of magnitude) when searching for the impulsive signature; these baryonic objects thus form an important background for our DM search. However, even when the mass of such bodies are comparable to the dark matter masses to which LISA is sensitive, at least two important differences aid in distinguishing the signals in the LISA data stream. First, the heliocentric velocities of the non-dark matter, gravitationally bound in the Solar System, will be generally smaller (by factors of several) than the dark population — this has the effect that the correlated peaks should have time-lags  $\sim 60$  hours for sun-orbiting objects, rather than  $\sim 6$  hr for Galactic DM. Second, and by far most important: non-dark matter reflects Sun light, so removing this background reduces to, literally, *looking* at it.

To make sure this is feasible, we estimate the brightness of such light-reflecting objects. The characteristic size of an asteroid with mass  $M$  and average density  $\bar{\rho}$  is,

$$R_c = 0.5 \text{ km} \left( \frac{M}{10^{15} \text{ gm}} \right)^{1/3} \left( \frac{\bar{\rho}}{3 \text{ gm cm}^{-3}} \right)^{-1/3}$$

The object size is  $\approx 0.6 \text{ km}$  for  $\bar{\rho} = 1 \text{ gm cm}^{-3}$ , appropriate for icy comets. If the object passes near LISA, then the bolometric flux of reflected light at Earth is,

$$f_{\oplus} \approx \frac{L_{\odot} R_c^2 r}{16\pi d_{\text{LISA}-\oplus}^2 d_{\text{LISA}-\odot}^2} \quad (2)$$

$$\approx 7 \times 10^{-11} \text{ erg s}^{-1}, \quad (3)$$

where  $L_{\odot}$  is the solar luminosity, a geometric/microphysical reflectance of  $r \approx 0.1$ , the LISA–Earth distance  $d_{\text{LISA}-\oplus} = 1 \text{ AU} \times \sin 20^\circ / \sin 80^\circ = 5.2 \times 10^{12} \text{ cm}$ , and the LISA–Sun distance

of  $d_{\text{LISA}-\odot} = 1$  AU. The flux will be radiated mostly at optical and infrared wavelengths. Assuming  $\sim 1/3$  (the precise number is not important) of the bolometric flux is radiated in the  $R$ -band filter ( $\lambda_c \sim 6000$  Å), the flux density in the  $R$ -band filter will be  $f_\nu \approx 6 \times 10^{-26}$  erg s $^{-1}$  Hz $^{-1}$  = 6 mJy or  $R \approx 14.5$  mag. These magnitude levels are routinely reached by small aperture, large field-of-view telescopes. LISA will subtend a field-of-view of no more than  $6^\circ$  in diameter, and always reside  $80^\circ$  from the Sun, observable for several hours per night. The next generation of near-earth asteroid surveys (e.g., PanSTARRS and LSST, starting in 2006) will patrol the sky  $\sim 10$  magnitudes fainter, cataloging asteroids at Earth-LISA distances which are smaller in size by a factor of  $\sim 100$ , or down to masses of  $\approx 10^9$  gm. If there is sufficient interest in understanding the local LISA gravitational background, the community might consider the benefits of launching a small ( $\sim 1$ -meter) optical telescope satellite in low-Earth orbit dedicated to observing the LISA field. If a reflecting object is found in monitoring, once the ephemeris is established and mass estimated, the effects upon the LISA baseline evolution can be calculated, removing the non-dark signal.

#### 4. Next-Generation Experiments

One of LISA's most obvious limitations as a DM detector is its measurement sensitivity, any improvement in which would increase the event rate significantly in both acceleration and impulse methods of detection. Another limiting factor is the correlation time; lengthening this would similarly improve detection rates in the impulsive channel. Of course, since these are the main limitations for LISA's gravity wave mission, they are already on the cutting-edge of feasibility, and so these are difficult levers to tweak.

A major limitation comes from the fact that LISA measures only tidal forces on the constellation, significantly decreasing the power in the signal. To get a sense for what an enormous limitation this is, consider Figure 1. The average deformation of the orbit of the constellation is  $\sim$ four orders of magnitude larger than the tidal displacement. Increasing the LISA arm-length will thus increase significantly the event rate. Since collisions with larger impact parameters have larger timescales, the finite correlation time tempers this improvement for large arm-lengths; nonetheless, this would lead to a significant improvement in resolution. This provides additional motivation for the construction of next-generation laser-interferometric gravitational observatories with larger baselines. Another glaring limitation of LISA is the cacophonous background of the visible solar system, whose signal on LISA is over 16 orders of magnitude larger than the signal we would like to measure. Moving this experiment, or a similar interferometer, outside the solar system would be a tremendous improvement (if technologically daunting). Incorporating such improvements into an



experimental design is beyond the scope of this letter; we will return to this issue in future work.

*Note added in manuscript:* As this *Letter* was being completed, we became aware of another group (Seto & Cooray 2004) who anticipated some features of the approach detailed above.

We would like to thank Nima Arkani-Hamed, Savas Dimopoulos, Matt Holman, Scott Hughes, Stephen Shenker, Matt Strassler and Matias Zaldarriaga for fruitful conversations. A.W.A. and J.S.B. are supported by Junior Fellowships from the Harvard Society of Fellows. This work was also supported by a research grant from the Harvard-Smithsonian Center for Astrophysics (J.S.B.) and a visiting position at the Rutgers High Energy Theory Center (A.W.A.).

## REFERENCES

- Afshordi, N., McDonald, P., and Spergel, D. N. 2003, Primordial Black Holes as Dark Matter: The Power Spectrum and Evaporation of Early Structures
- Alcock, C. *et al.* 2001, *Astrophys. J.*, 550, L169
- Arkani-Hamed, N., Dimopoulos, S., and Dvali, G. R. 1999, *Phys. Rev. D*, 59, 086004
- Bender, P. *et al.* 1998, Laser Interferometer Space Antenna (LISA) for the detection and observation of gravitational waves: Pre-Phase A Report, 2nd edn., LISA Study Team, <http://www.srl.caltech.edu/lisa/documents/PrePhaseA.pdf>
- Bertone, G., Hooper, D., and Silk, J. 2004, Particle dark matter: Evidence, candidates and constraints
- Blumenthal, G. R., Faber, S. M., Primack, J. R., and Rees, M. J. 1984, *Nature*, 311, 517
- Carr, B. 1994, *Ann. Rev. Astr. Ap.*, 32, 531
- Carr, B. J. and Hawking, S. W. 1974, *Mon. Not. R. astr. Soc.*, 168, 399
- Clancy, D., Guedens, R., and Liddle, A. R. 2003, *Phys. Rev. D*, 68, 023507
- Cornish, N. J. and Rubbo, L. J. 2003, *Phys. Rev. D*, 67, 022001

- Davis, M., Efstathiou, G., Frenk, C. S., and White, S. D. M. 1985, *Astrophys. J.*, 292, 371
- de Bernardis, P. *et al.* 2000, *Nature*, 404, 955
- Gates, E. I., Gyuk, G., and Turner, M. S. 1995, *Astrophys. J.*, 449, L123
- Griest, K. 1995, The nature of the dark matter, astro-ph/9510089
- Gron, O. and Soleng, H. H. 1996, *Astrophys. J.*, 456, 445
- Hagmann, C. *et al.* 1998, *Physical Review Letters*, 80, 2043
- Hawking, S. 1971, *Mon. Not. R. astr. Soc.*, 152, 75
- Hawking, S. W. 1975, *Commun. Math. Phys.*, 43, 199
- Lewin, J. D. and Smith, P. F. 1996, *Astroparticle Physics*, 6, 87
- Paczynski, B. 1986, *Astrophys. J.*, 304, 1
- Seto, N. and Cooray, A. 2004, astro-ph/0405216
- Tremaine, S. 1992, *Physics Today*, 45, 28
- Zwicky, F. 1933, *Helv. phys. Acta*, 6, 110

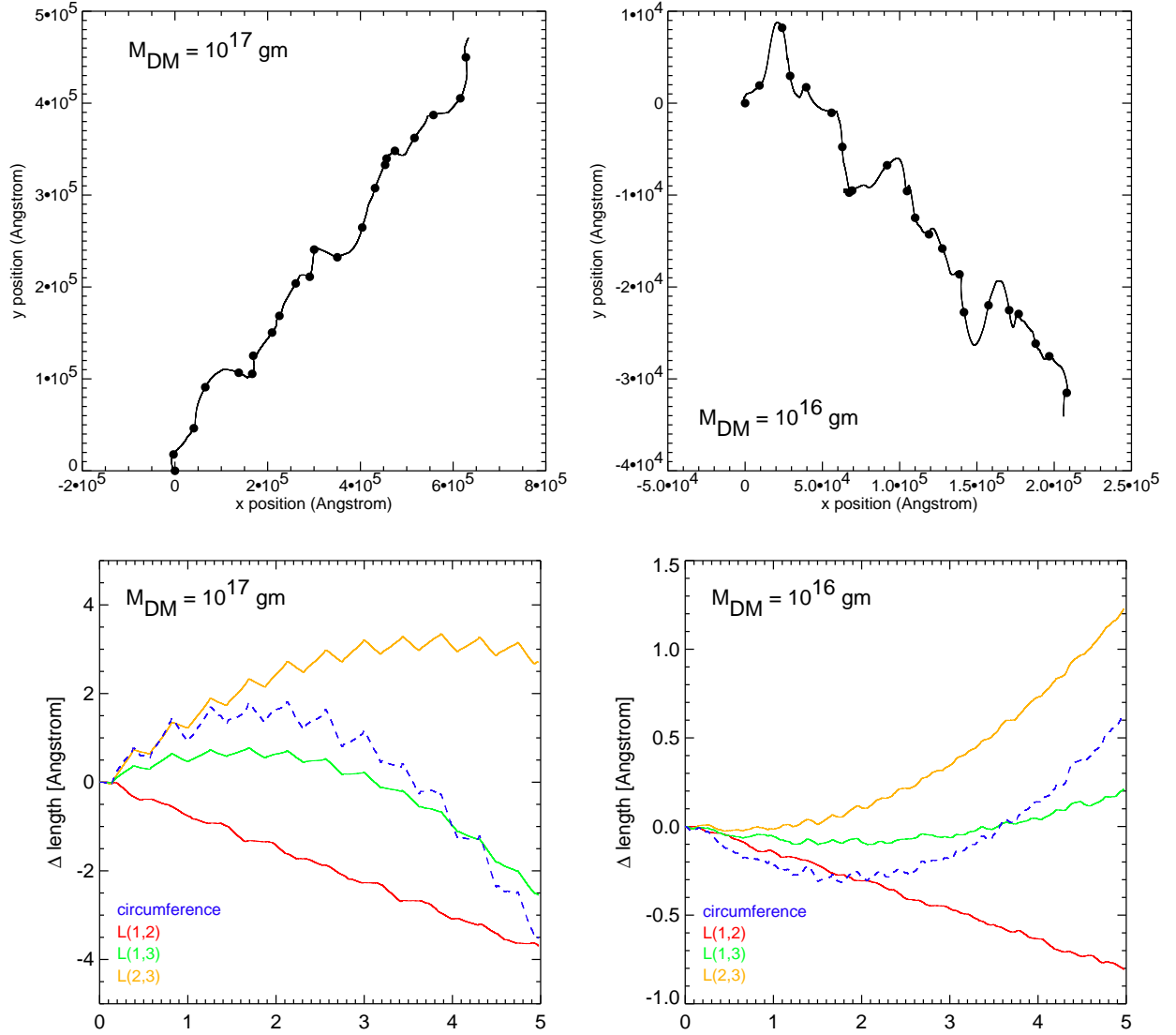


Fig. 1.— (top) Quasi-Brownian walk of a single station from Keplerian orbit, perturbed only by DM objects of mass  $M_{\text{DM}} = 10^{17}$  (left) and  $M_{\text{DM}} = 10^{16}$  (right) over five years. The filled circles are placed at 3 month intervals. As expected, the total scale of the motion depends linearly on the dark matter mass. (bottom) Distance between stations ( $L[i, j]$ ) as a function of time, significantly smaller than the bulk motion of the individual stations. The apparent periodicity in the impulse signal is due to periodic boundary conditions in the DM simulation.

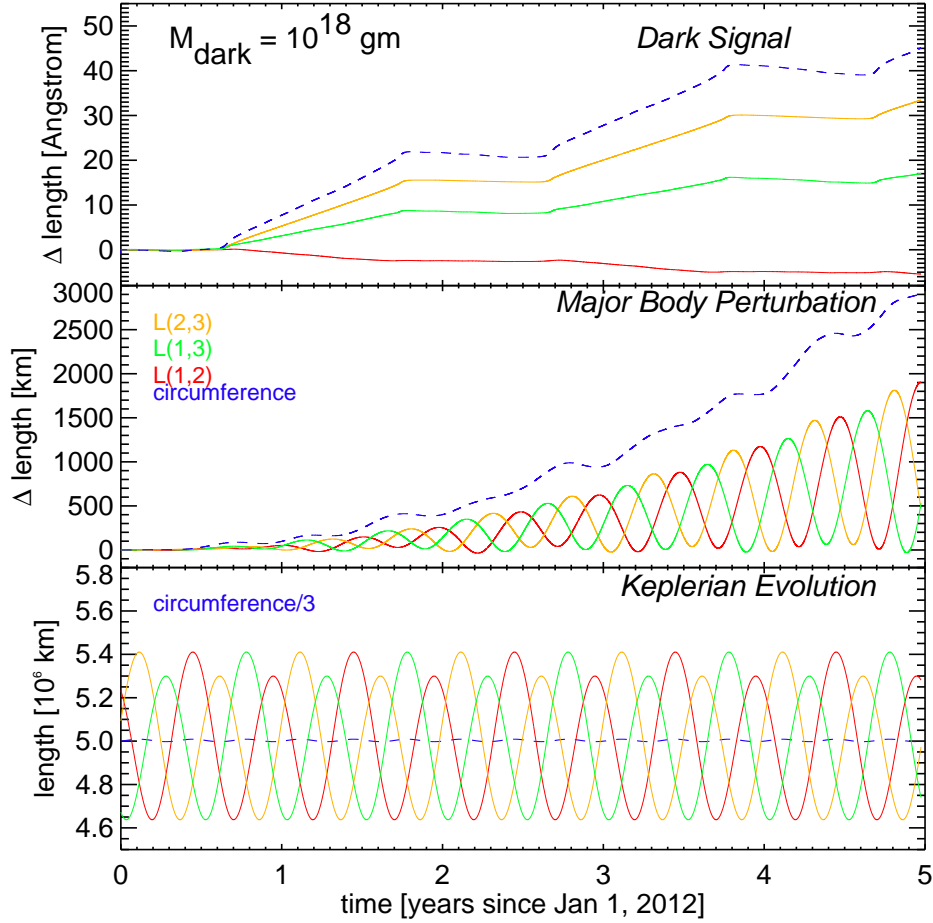


Fig. 2.— Simulation of inter-station distances in the presence of  $M_{\text{DM}} = 10^{18} \text{ gm}$  dark matter, including the orbit of the LISA constellation and perturbations from all inner solar system major bodies. The vast range of scales inherent in this dark matter detection technique is readily apparent.

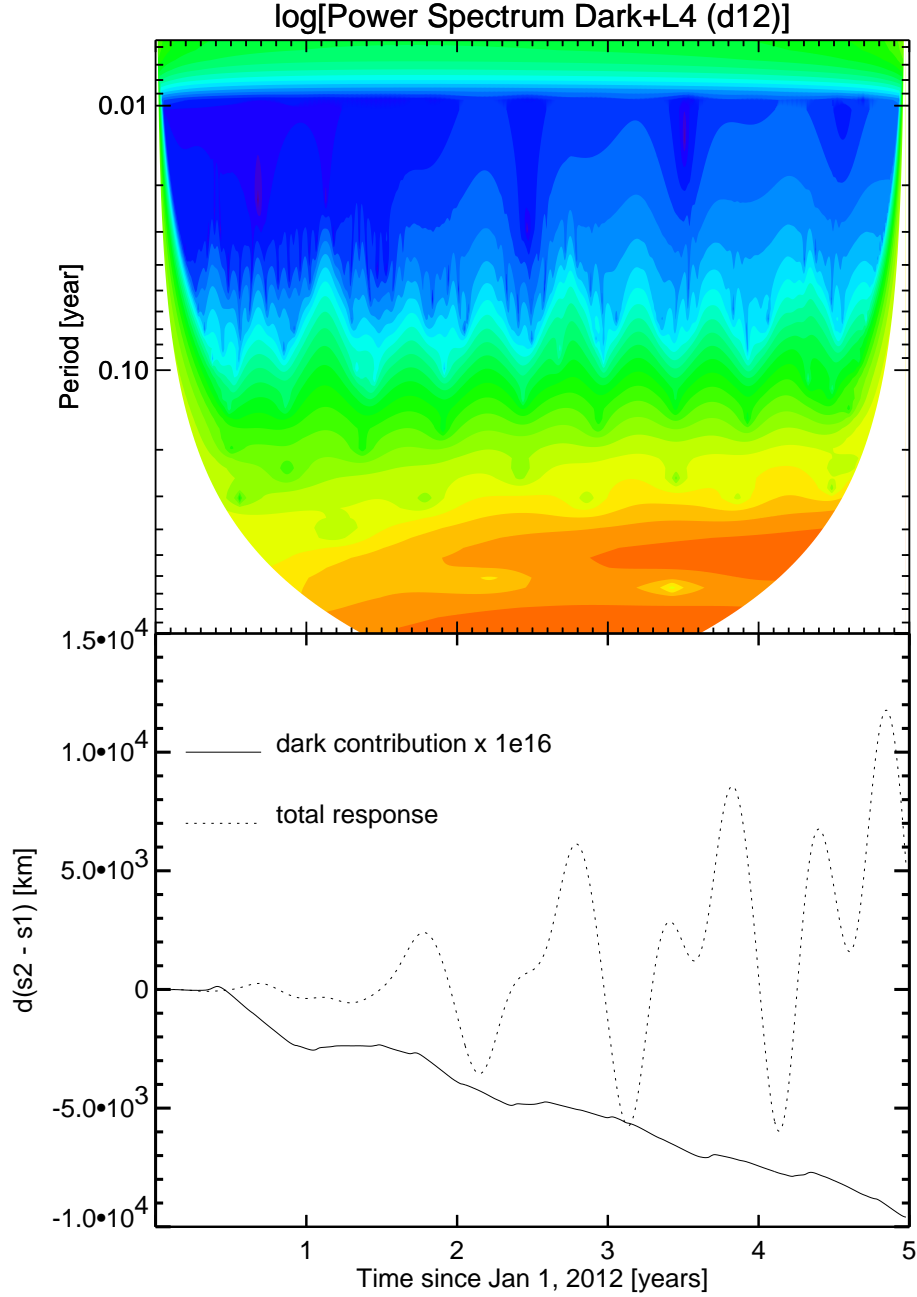


Fig. 3.— (top left) Time evolution of the power-spectrum of inter-station distances for the LISA orbit, determined by wavelet transform. Relative power increases from blue to red. Orbital perturbations due to all major Solar System bodies are included. Earth, which dominates the perturbations, has been excluded to retain a dynamic range of the DM and major body perturbations less than  $10^{16}$ , the numerical precision of double floating point numbers. The contribution from the Moon is manifested in the short period spikes every 28 days. (bottom) The time evolution of the inter-station distance (dotted line) and the contribution of from the dark matter in the simulation. Here we simulated 35 DM objects with  $M_{\text{DM}} = 10^{18}$  gm streaming in the inner 11 AU of the Solar System.

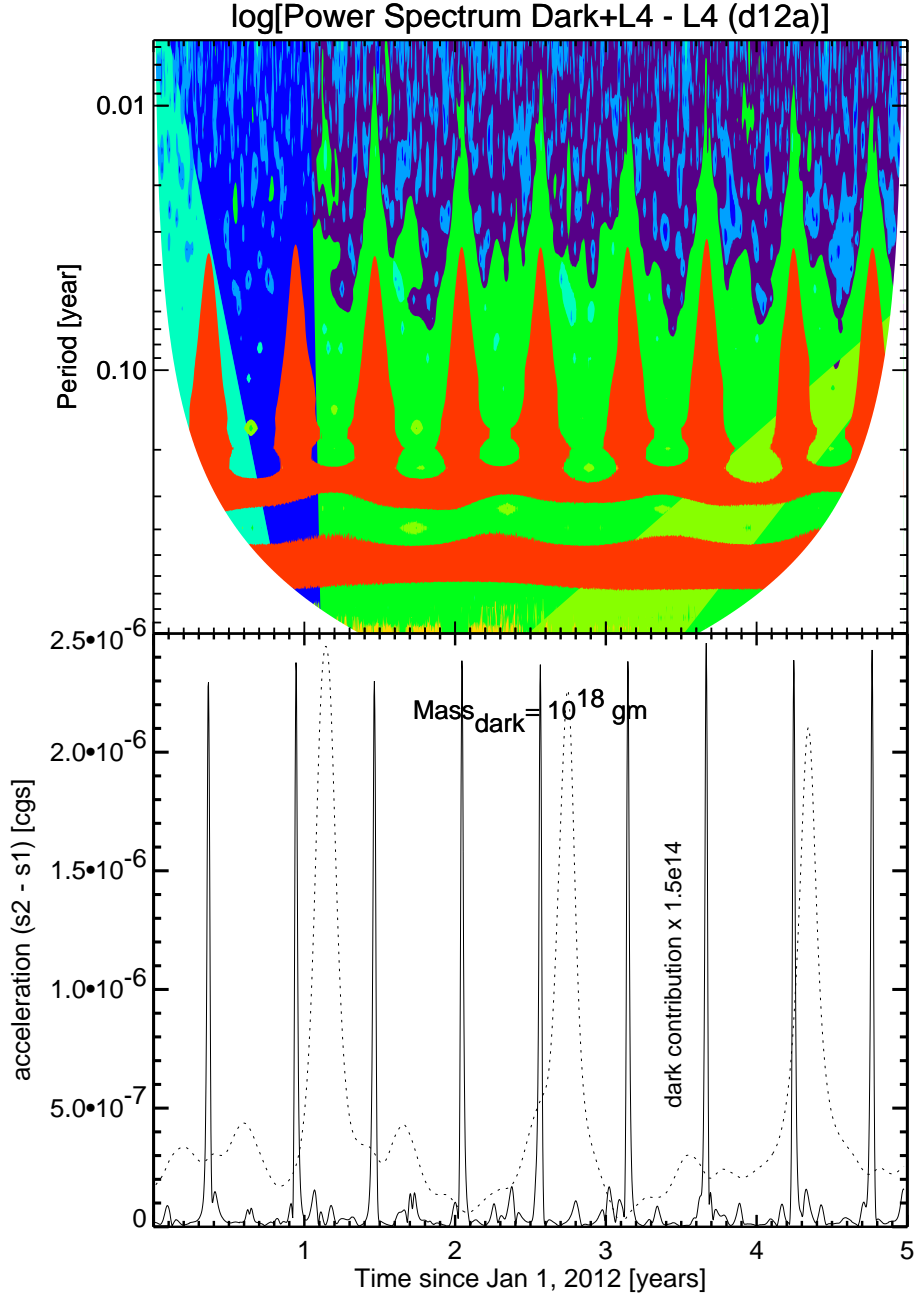


Fig. 3.— (continued) (top right) Demonstration that DM can be detected in the presence of significantly larger perturbations: time evolution of the power-spectrum of the difference between the inter-station acceleration with and without DM. The spikes from the DM signal are readily seen; the apparent periodicity is due to periodic boundary conditions in the simulation. The large blue cone in the first year is an artifact of the dynamic range in the relative precision on the two acceleration scales (bottom right) The time evolution of the total inter-station acceleration (dotted line) and the contribution of from the dark matter in the simulation (solid line).

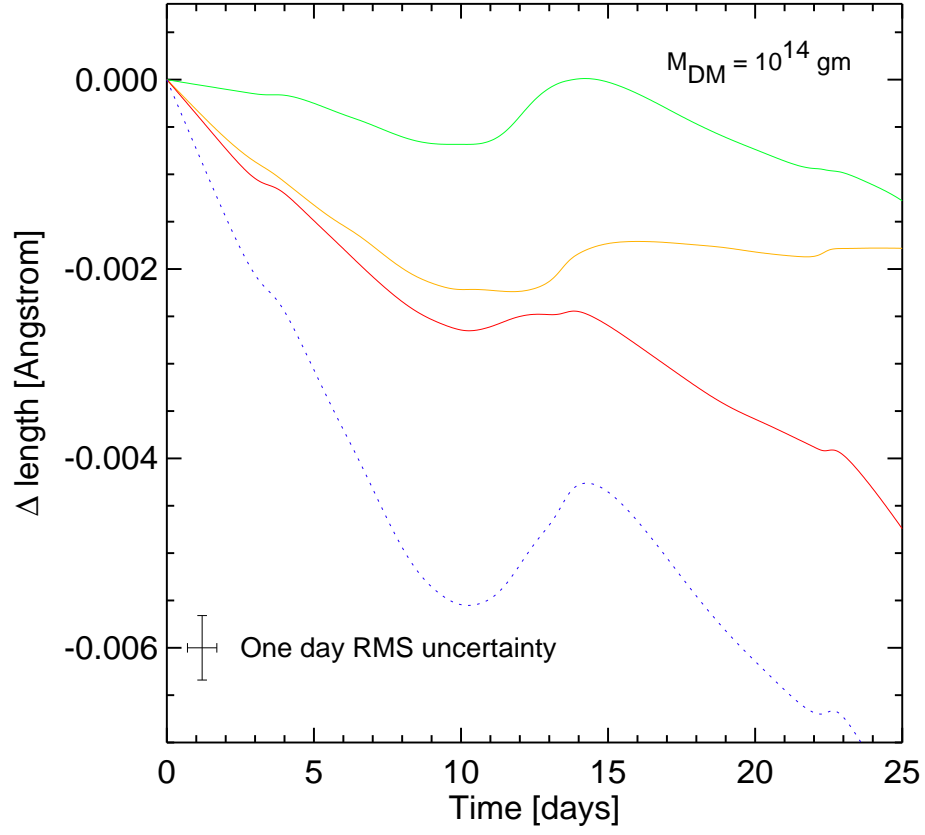


Fig. 4.— Zoom in on a generic DM passage event that occurred in a simulation with 2000  $M_{\text{DM}} = 10^{14} \text{ gm}$  objects. Events generated by  $M_{\text{DM}} = 10^{14} \text{ gm}$  DM will produce detectable signals, if the decorrelation timescale is longer than several days (as currently anticipated).